Desalination and Water Treatment
www.deswater.com

doi: 10.5004/dwt.2020.26285

204 (2020) 438–448
November

Engineering superhydrophobic-superoleophilic nylon mesh for high-efficiency oil-water separation

Hong Shi[a,*], Tiantian Wang[b], Long Zhao[a], Weihua Zhu[a,*]

[a]*School of Chemistry and Chemical Engineering, Jiangsu University, Zhenjiang 212013, P.R. China, Tel. +86-0511-88791928; emails: hshi@ujs.edu.cn (H. Shi), sayman@ujs.edu.cn (W.H. Zhu), longzhao@ujs.edu.cn (L. Zhao)*
[b]*School of Chemistry, Chongqing Normal University, Chongqing 401331, P.R. China, Tel. +86-023-6536277; email: gbzhou@cqnu.edu.cn (T.T. Wang)*

Received 23 December 2019; Accepted 16 June 2020

ABSTRACT

With the aggravation of environmental pollution caused by oil and chemical leakages, oil-water separation has attracted great attention from both academia and industry. In this paper, a cost-effective dip-coating and thermal treatment method based on the modification of nylon mesh has been developed for oil-water separation. Ultra-low surface energy polybenzoxazine and hydrophobic silica nanoparticles were adopted to engineer nylon mesh superhydrophobic-superoleophilic. The morphology, chemical composition and surface properties of the modified nylon mesh were characterized by using scanning electron microscopy, Fourier-transform infrared spectroscopy and contact angle (CA) measurements, etc. The modified nylon mesh exhibited excellent superhydrophobic property with a high water contact angle of 154.3° and distinct superoleophilic feature with a negligible oil CA of nearly 0°, leading to more than 99.5% ± 0.1% of oil-water separation efficiency with high permeate flux (up to $1.77 \times 10^4 \pm 100$ L/(m^2 h)) merely under gravity. In addition, the novel nylon mesh displayed excellent reusability after more than 30-cycle measurements. Our findings may provide a promising approach to the treatment of oil spills and oily wastewater.

Keywords: Oil-water separation; Superhydrophobic; Superoleophilic; Nylon mesh

1. Introduction

Oil-water separation has attracted numerous attention due to serious oil pollution in the petrochemical industry, such as oil spill accidents and oily wastewater discharge [1–3]. Exploring functional materials to effectively separate the mixture of water and oil is still quite a challenging topic [4–6]. Due to specific oil-water separation requirements, various materials like cellulose fibers [7,8], metal wires [9], carbon fibers [10], electro-spinning fibers [11,12], metal meshes [13–15], porous sponges [16,17], carbon nanotubes [18] and biomass carbon aerogel [19–21] have been selected to construct the target practical materials. A few important criteria in selecting the skeletons include material cost, separation efficiency, capacity, material reusability and environmental requirements [22,23].

Some polymers, for instance, polyamides, are usually cheap, flexible, light mass and high specific strength, which meet the criteria for building the oily water separation membranes. Nylon, as one of the polyamides, has been reported to be successfully applied in oil removal. For example, Zhang et al. [24] decorated polydivinylbenzene onto different porous substrates including nylon mesh and found that all these materials were able to separate oil/seawater mixtures with ultrahigh efficiency. Chen et al. [25] adopted plasma to treat nylon mesh for fabricating super-wettability materials and found that the separation efficiency can

* Corresponding authors.

be above 97.5% for various oil/water mixtures. Shang et al. [26] demonstrated several commercial materials with modified superhydrophobic surfaces showing excellent separation performance for collecting various oils/organic solvents from water. Li and Zhang [27] coated silica particles and polystyrene on nylon cloth for oil/water separation and found that oil could be separated from the oil-water mixture rapidly through this membrane without any extra force. These previous reports indicated that nylon materials can achieve sufficient oil/water separation, however, with either harmful chemicals or complex fabrication processes. Therefore, finding a proper material with environmentally friendly and simple treatment for decorating nylon skeleton is highly desired.

Polybenzoxazine (PBz) possessing ultra-low surface energy without fluorine and silicon atoms is promising for a stable superhydrophobic surface due to its environmentally friendly, low cost and high thermal stability, etc. [28,29]. A few prosperous superhydrophobic surfaces using polybenzoxazine composites have been reported recently, for example, crosslinked PBz-based dense membranes for pervaporation [30], electrospun nanofiber mats for oil-water separation [31] and separators for lithium-ion batteries [32].

Herein, we have employed nylon mesh as the membrane substrate and polybenzoxazine as the main coating material to endow the surface with the property of superhydrophobic and superoleophilic. Silica nanoparticles (SiO_2 NPs) were also introduced to the surface in order to increase surface roughness, which is crucial for superwettability. A simple dip-coating and thermal treatment procedure have been exploited as shown in Fig. 1. Material characterization and oil-water separation measurements have been carried out to investigate the property and the potential utility of this novel nylon mesh.

2. Materials and methods

2.1. Materials

Nylon mesh (120 mesh size) was purchased from Shanghai Hongxiang Metal Mesh Co., Ltd., (China). Reagents including SiO_2 NPs (Aerosil R812S, hydrophobic, particle size < 7 nm, fumed, spherical), paraformaldehyde, dodecyl amine, phenol, anhydrous sodium sulfate, sodium hydroxide, hydrochloric acid, ethyl acetate, acetone, oil red O, methylene blue and chloroform were obtained from Aladdin Chemistry Co., Ltd., (China). All chemicals were of analytical grade and used as received without further purification. Ultrapure water was produced by a Milli-Q Biocel unit (Millipore, USA) with the resistivity of 18 M Ω cm and was used in all experiments.

2.2. Instrumental characterization

Water contact angles (WCA) of nylon meshes were measured with an instrument (Model: CM200) from KSV Instruments Ltd., Finland. The reported static contact angles represent the average of five measurements at different areas of surfaces. The micro-texture and morphologies were analyzed by scanning electron microscopy (SEM; JSM-7001F, JEOL, Japan). Fourier-transform infrared spectroscopy (FTIR) spectra were recorded using a Perkin Elmer 1430 (USA), in the wavenumber range 4,000–400 cm^{-1} with attenuated total reflectance (ATR) mode. Proton nuclear magnetic resonance (^1H NMR) spectroscopy was performed using a German Bruker AVANCE II at a proton frequency of 400 MHz to characterize the chemical structure of the benzoxazine monomer (Bz). Water content was measured with a Karl Fischer Moisture Titrator (MKC-510B) from Kyoto Electronics Manufacturing (Japan). Stress-strain curves of the nylon meshes were recorded using an INSTRON CMT4104 mechanical tester (China) with a sample size of 1 cm × 3 cm and an elongation rate of approximately 0.5 mm min^{-1}.

2.3. Synthesis of benzoxazine monomer

Bz was synthesized using dodecylamine, phenol and paraformaldehyde through the Mannich reaction according to the literature [33]. In detail, dodecylamine and phenol with a molar ratio of 1:1 were mixed into a 250 mL three-neck flask. The mixture was heated to 80°C and kept for another 10 min in an oil bath. Subsequently, 0.11 mol of paraformaldehyde was added into the solution with vigorous stirring upon further heating up to 110°C. After 2 h reaction, the crude product was dissolved in ethyl acetate and washed with sodium hydroxide solution (2 M) twice and water three times. After drying in anhydrous sodium sulfate overnight, the products were filtered and distilled to obtain the Bz. The Bz obtained was yellowish and viscous. The chemical structure of the Bz was confirmed by FTIR and ^1H NMR spectroscopy. FTIR spectra (ATR mode), cm^{-1}:930.61 (O–C–N), 1,047.34 (symmetric stretching, C–O–C), 1,239.44 (asymmetric stretching, C–O–C) and 1,372.51 (wagging, oxazine, CH_2), 1,742.32 (stretching vibration, C=O of solvent ethyl acetate).

2.4. Modification of nylon mesh

The fabrication process of the modified nylon mesh is illustrated in Fig. 1. First of all, the nylon mesh was cut into a circular shape (diameter 4.5 cm). Then it was cleaned with acetone and ultrapure water for 30 min successively by using an ultrasonic cleaner. After that, it was dried in an oven at 60°C for 30 min to remove the moisture completely. In the typical dip-coating process, Bz (1.5 g, 7.7 wt.%) was completely dissolved in ethyl acetate (20 mL), followed by dispersing SiO_2 NPs (0.25 g, 1.4 wt.%) into the solution at ambient temperature. The raw nylon mesh was thereafter dip-coated by the mixture for 15 min under ultrasonic agitation and then dried at 60°C for 30 min to remove the solvent and cured at 200°C for 1 h. Eventually, the superhydrophobic and superoleophilic nylon mesh was obtained by this one cycle dip-coating and thermal treatment procedure. The free-standing modified nylon mesh was applied for measurements and oil-water separation tests directly.

2.5. Oil-water separation

For oil-water separation measurement, the modified nylon mesh was horizontally fixed with a stainless steel clamping device. The gravity-driven separation was achieved by slowly adding 10 mL of water and 10 mL of oil

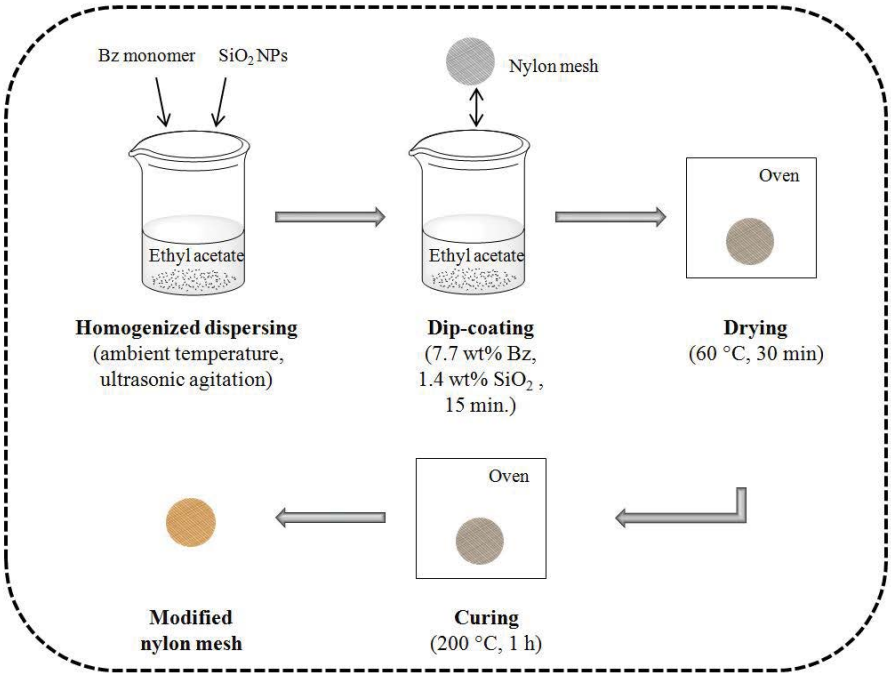

Fig. 1. Modification process of the superhydrophobic–superoleophilic nylon mesh.

successively into the upper glass tube. The separated oil was collected from the bottom tube to evaluate the separation efficiency. For better visualization, oil and water were dyed with oil red O and methylene blue, respectively.

The separation efficiency was measured according to the following equation [7]:

$$\eta = \left(\frac{V_a}{V_0}\right) \times 100\% \quad (1)$$

where η is the separation efficiency, V_0 (L) and V_a (L) are the volume of the original oil and collected oil after separation, respectively.

The flux was measured according to the following equation [20]:

$$J = \frac{V}{(t \times A)} \quad (2)$$

where J is the flux (L/(m^2 h)), V is the volume of the collected oil (L), t is the time used for collecting the oil (h), and A is the effective area of the modified nylon mesh (8.1×10^{-4} m^2).

3. Results and discussion

3.1. Morphology and chemical composition

Fig. 2 shows the SEM images of the nylon mesh before and after modification. It is clearly shown that the mesh skeleton well maintains its porous structure after surface modification. The original nylon mesh is composed of microfibers with 90 to 100 μm in diameter showing a smooth fiber surface (Fig. 2a), while the pore size stays unchanged but the surface changes pretty rough after modification (Fig. 2b). The SiO_2 NPs were aggregated and form a hierarchical structure with many deep grooves on the fabric surface as shown in high magnification images. Although the size of SiO_2 NPs is about 7 nm provided by the supplier (Fig. 2e), the depths of grooves are in a few microns range and the average thickness of SiO_2 NPs film is about 2 μm. These deep grooves will trap air at oil/water mixtures-nylon mesh interfaces and then prevent water to penetrate into the nylon mesh, creating a hydrophobic surface. Although the PBz cannot be seen from SEM image and hence its thickness cannot be estimated, the FTIR measurement, as discussed in the next section, proves the doping of it onto the surface of SiO_2 NPs and nylon fabric.

The energy-dispersive X-ray spectroscopy (EDS) test was further carried out to identify the chemical composition of the original and modified nylon mesh (Fig. 3). In Fig. 3a, elements C, N and O were detected as the components of original nylon mesh as prepared from polyamide. After the modification, the silica (Si) atom was observed with a percentage of about 2.82% in the mesh. Additionally, the percentage of oxygen (O) atom of modified nylon mesh increases as compared to the original counterpart. The appearance of the Si atom and the increase of O percentage further implies the successful coating of silica particles. It is noted that each sample showed a clear peak of Au, which is caused by the golden spraying to increase the surface conductivity of the nylon mesh.

The EDS elemental mapping of the modified nylon mesh in Fig. 3b clearly shows a homogeneous distribution of the C, N, O and Si elementals onto the surface of whole modified nylon mesh.

The synthesis procedures of Bz and its polymer are illustrated in Fig. 4. The chemical structure of the Bz was confirmed by ^{1}H NMR spectroscopy as shown in Fig. 5.

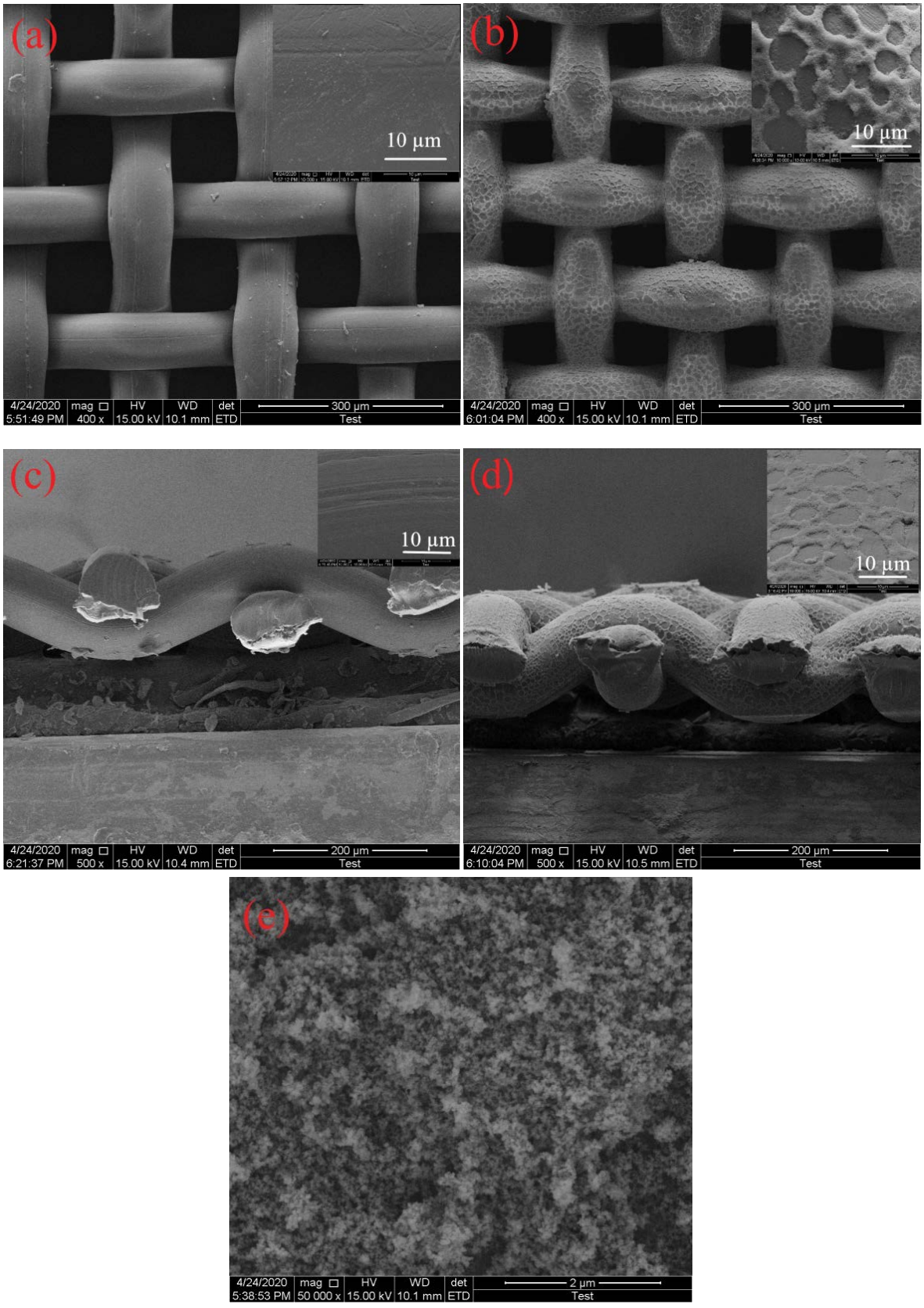

Fig. 2. Surface SEM images of (a) original nylon mesh, (b) modified nylon mesh, (e) SiO_2 NPs. Cross-sectional SEM images of (c) original nylon mesh and (d) modified nylon mesh. The insets show the corresponding high magnification image of each sample.

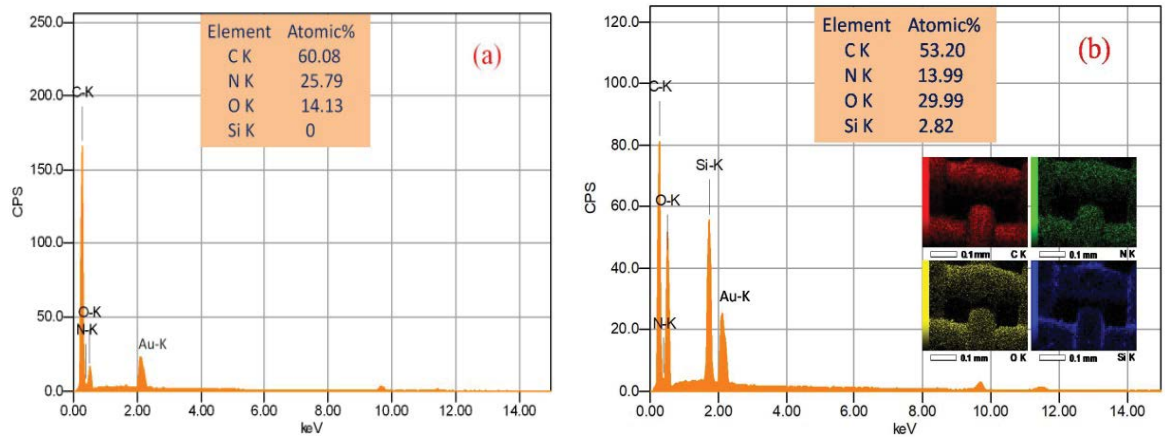

Fig. 3. EDS analysis of (a) original and (b) modified nylon mesh. The inset in (b) shows the EDS elemental mapping images of modified nylon mesh.

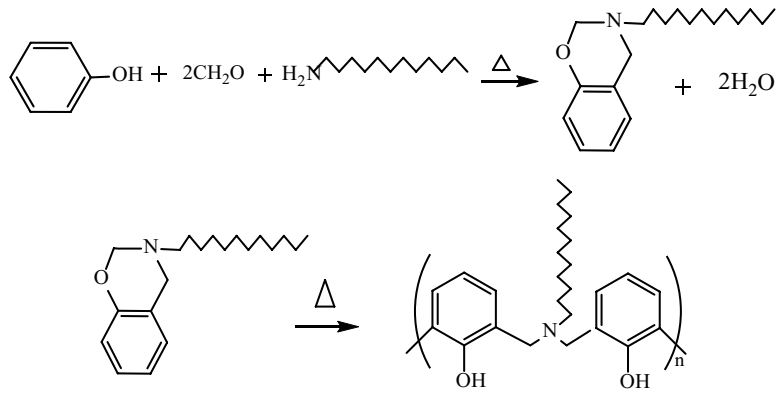

Fig. 4. The synthesis procedure of pendant aliphatic chain-substituted benzoxazine monomer and its polymer.

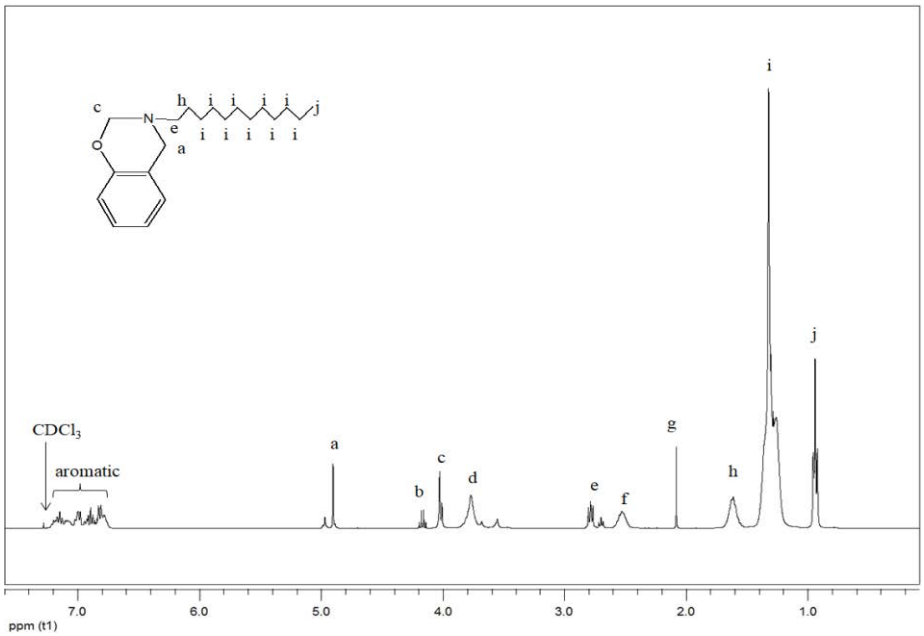

Fig. 5. ^{1}H NMR spectroscopy of the benzoxazine monomer (δ = 0.89 (*t*, 3H; –CH_2–$(CH_2)_{10}$–CH_3), 1.25 (*m*, 18H; –CH_2–CH_2–$(CH2)_9$–CH_3), 1.53 (*m*, 2H; –CH_2–CH_2–$(CH_2)_9$–CH_3), 2.73 (*t*, 2H; –CH_2–$(CH_2)_{10}$–CH_3), 3.99 (*s*, 2H; Ar–CH_2–N, oxazine ring), 4.86 (*s*, 2H; O–CH_2–N, oxazine ring), 6.76 (*d*, 1H), 6.85 (*t*, 1H), 6.96 (*d*, 1H), and 7.11 (*t*, 1H).(b,d,f,g in Fig. S1 represent impurity)).

The FTIR spectrum of Bz in Fig. 6a shows characteristic absorption bands at 930.61 cm^{-1} (stretching vibration of O–C–N), 1,047.34 cm^{-1} (symmetric stretching of C–O–C), 1,239.44 cm^{-1} (asymmetric stretching vibration of C–O–C), and 1,372.51 cm^{-1} (wagging, oxazine, CH_2) assigning to the oxazine ring. This spectrum is very similar to the reported one by Zhang et al. [34]. The results confirm the chemical constitution of Bz. Benzoxazine polymer (PBz) was obtained after thermal curing at 200°C for 1 h. Upon curing at 200°C, the *in situ* polymerization of Bz monomers leads to the formation of the Mannich bridge cross-linked structure, and finally generating a cured thermosetting PBz layer on the fiber surface. It is noticed that the out-of-plane O–C–N bending vibration at 930.61 cm^{-1} and the symmetric stretching vibration of C–O–C bond at 1,047.34 cm^{-1} is not observed in the FTIR spectrum of PBz (Fig. 6b), which confirms the opening of the oxazine ring and the polymerization reaction. In addition, the appearance of a very weak absorption band at 1,240.21 cm^{-1} (asymmetric stretching, C–O–C) in Fig. 6b may due to the incomplete polymerization reaction.

The successful modification was also examined by the FTIR spectrum of pristine and modified nylon mesh. Compared with Fig. 6c of the pristine nylon mesh, Fig. 6d shows new absorption bands appeared at 1,106.94 cm^{-1} assigning to characteristic absorption bands of SiO_2 (asymmetric stretching, Si–O–Si, Fig. 6e), and 1,241.13 cm^{-1} assigning to incompletely polymerized PBz (asymmetric stretching, C–O–C).

3.2. Wettability

To investigate the surface wettability of the original and modified nylon mesh, the WCA of each nylon mesh was measured. Fig. 7 displays the morphology of water droplets on different nylon meshes. The WCAs of original and modified nylon meshes are 118.2° and 154.3°, respectively. The increased degree of contact angle (CA) demonstrates a superhydrophobic property of the modified nylon mesh.

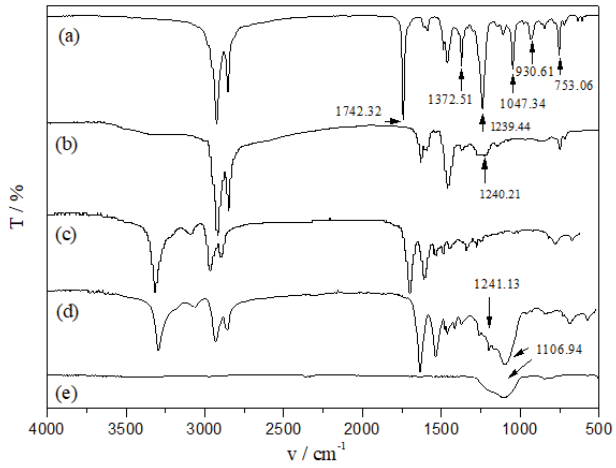

Fig. 6. FTIR spectra of (a) Bz, (b) PBz, (c) pristine nylon mesh, (d) modified nylon mesh and (e) SiO_2 NPs.

In general, both surface rough structure and low surface free energy chemical composition are beneficial for a superhydrophobic surface. In terms of this modification procedure, silica nanoparticles increase the roughness of the nylon mesh surface and polybenzoxazine decreases the nylon mesh surface energy. The synergistic effect consequently results in the enhancement of hydrophobicity.

Fig. 8a shows the time-lapse images of a water droplet contacting the modified nylon mesh in air. An about 8 μL water droplet deposited on the modified mesh can be easily picked up by a microsyringe, and the suspended droplet can move up and down in between the tip of the syringe and the nylon mesh for many cycles, indicating a superhydrophobic property of the modified mesh. Fig. 8b shows the time-lapse images of an oil (chloroform) droplet contacting the modified nylon mesh. The droplet was absorbed by the mesh and quickly spread and then permeated through it within 0.1 s with a water CA of about 0°, indicating a superoleophilic property of the modified nylon mesh.

Furthermore, the surface wettability of nylon meshes was investigated using visual images. In order to observe clearly, water was dyed using methylene blue (blue), while oil was dyed using oil red O (red). Fig. 9 shows apparently that the droplets of oil spread out on both the original and modified nylon mesh surface, while water droplets stay steady on the surface of both the original and modified nylon mesh. It is also observed that the water droplet on the modified nylon mesh is more spherical than that on the original nylon mesh, which proves the assumption that the modification alters the mesh properties to be superhydrophobic. In addition, the color changes of pristine nylon mesh from white to yellow suggests the coverage of yellowish PBz on its surface.

3.3. Water intrusion pressure

For an effective oil-water separation process, the liquid (water) intrusion pressure is one of the important requirements in order to avoid the water passage. The intrusion pressure (P_{max}) of the nylon mesh was calculated using the following equation [35]:

$$P_{max} = \rho g h_{max} \quad (3)$$

where ρ is the density of the water, g is the acceleration of gravity, and h_{max} is the maximum height of water that mesh can support.

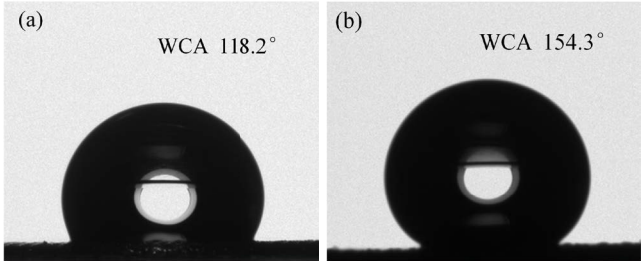

Fig. 7. WCA of different nylon meshes: (a) original and (b) modified.

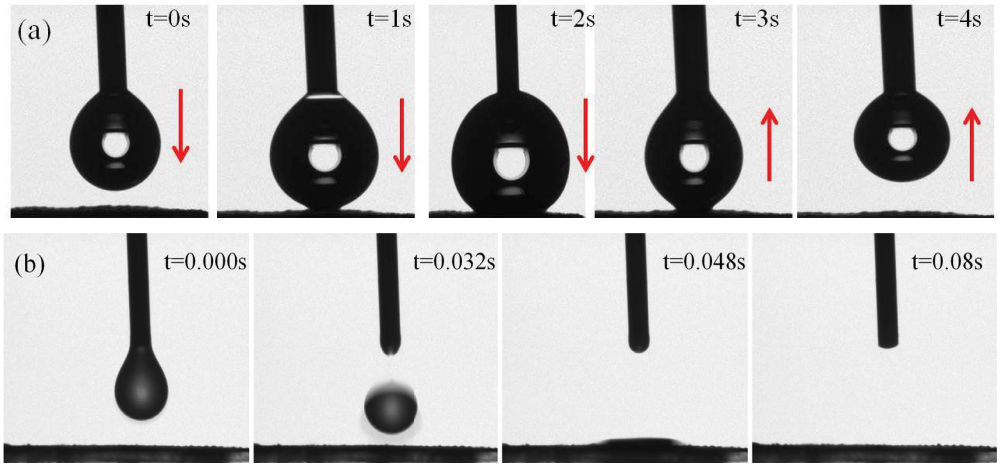

Fig. 8. (a) Water droplet making and losing contact with a modified nylon mesh and (b) time-lapsed snapshots of chloroform droplets contacting with a modified nylon mesh.

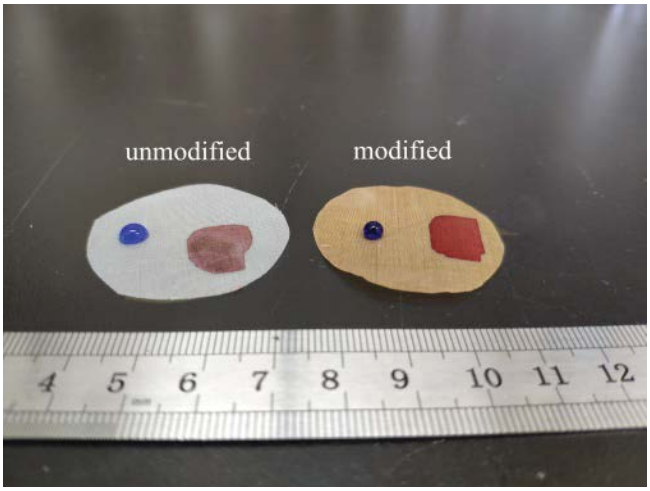

Fig. 9. Optical image of drops of water (blue color) and oil (red color) deposited on nylon meshes.

The maximum bearable height of the modified nylon mesh is found to be about 15 cm (Fig. 10). The calculated intrusion pressure is 1.15 kPa, under which water cannot flow through the mesh. On the contrary, the maximum bearable height of the unmodified nylon mesh is about 5 cm, which is three times lower than that of the modified nylon mesh. It indicates that the modified nylon mesh has excellent separation ability since oil can permeate through it within 0.1 s.

3.4. Separation efficiency and reusability

Pristine nylon mesh did not show satisfactory water resistance and oil-water selectivity as water could permeate gradually through it. Hence, the separation of oil-water with the modified nylon mesh was carried out. Chloroform was used as an exemplar of oil rather than some other oils since chloroform-contained wastewater is commonly discharged from industry [20,21,36,37].

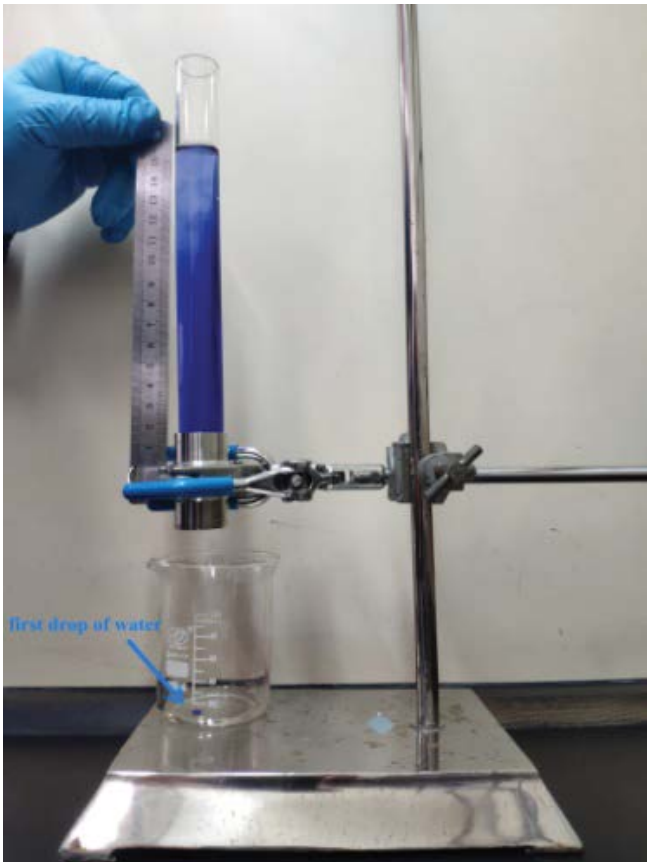

Fig. 10. Water-intrusion pressure of the modified nylon mesh (water was dyed with methylene blue).

The oil-water separation experiment procedure is shown in Fig. 11. Oil quickly permeate through the modified nylon mesh and flow into the beaker underneath due to the superoleophilicity. Meanwhile, water is unable to penetrate the sample and remain at the top because of the

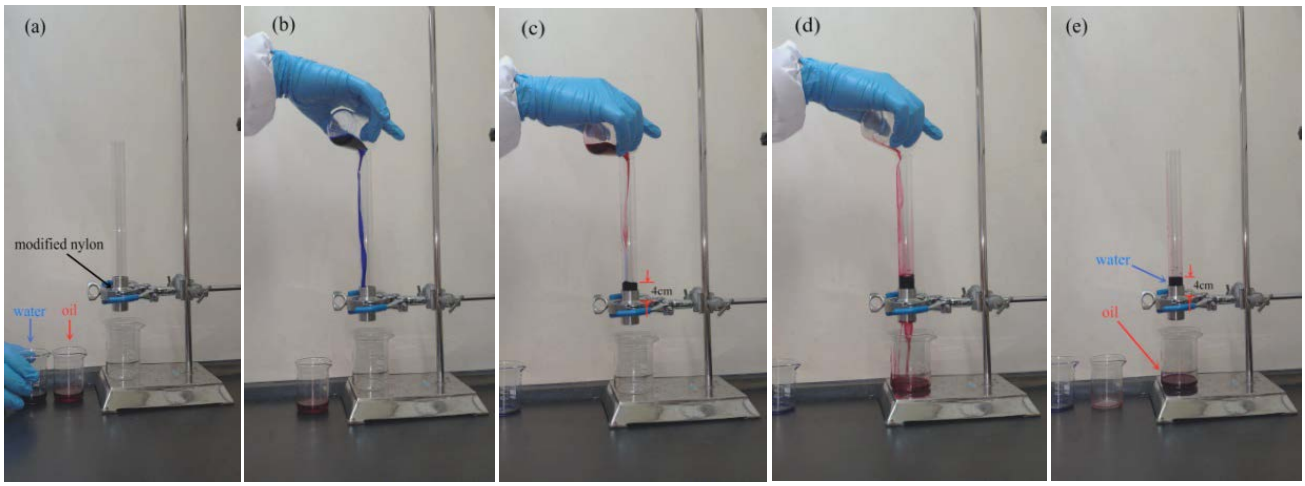

Fig. 11. Photographs of the oil-water separation process for the modified nylon mesh.

superhydrophobic. After the separation process, the water content in the separated oil was measured, which was similar to the solubility of water in chloroform (560 ppm at 25°C). The calculated separation efficiency value reaches 99.8% ± 0.1% and corresponding flux is 1.77 × 10^4 ± 100 L/(m^2 h). These values are much greater than a few recently developed superhydrophobic membranes that separate chloroform/water mixture. For instance, a cellulose/layered double hydroxide membrane achieved the separation efficiency and flux of 95.0% and 4,986 L/(m^2 h), respectively [7,35].

It is worth noting that no external force was employed during the fast separation process (within 8 s), but only with its own weight. The results indicate that the modified nylon mesh is a promising candidate in industrial oil-polluted water treatments and oil spill clean-up.

Another important consideration of selective separation application is reusability. To examine the reusability of the modified nylon mesh, the separation test mentioned above was repeated for 30 cycles. During the tests, the mesh was recovered by water-rinsing and drying at 100°C for 30 min. The mesh retained an ultrahigh oil permeation flux (1.8 × 10^4 ± 100 L/(m^2 h)) and high separation efficiency (above 99.5% ± 0.1%) after the 30-cycle tests (Fig. 12), implying the outstanding stability of the resultant nanosphere coating. SEM micrograph showing no obvious changes in the skeleton and abundant nanospheres on the nylon mesh surface further demonstrates the stability of the nanosphere coating.

In addition, the stability of the modified nylon mesh was investigated in different solutions with pH 4, 7 and 10. The WCA of the modified nylon mesh after immersing is shown in Fig. 13. After 24 h, the WCAs of the modified nylon meshes decreased to 151.9°, 152.3° and 149.6° in pH 4, 7 and 10, respectively. Despite the slight decrease of the WCA, all of the immersed nylon meshes still exhibit hydrophobic. This result implies that the modified nylon mesh can effectively function in the acidic, alkaline and neutral environments for a relatively long time (24 h),

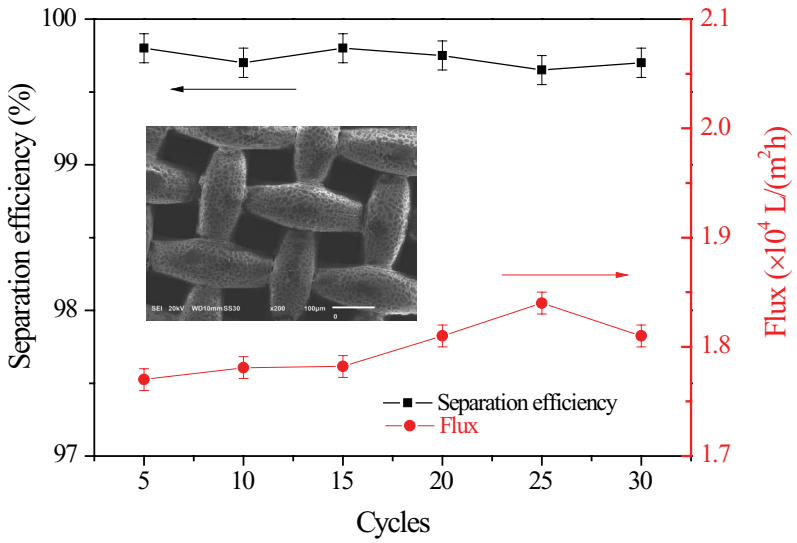

Fig. 12. Reusability of modified nylon mesh. The inset shows the SEM image of the modified nylon mesh after 30-cycle tests.

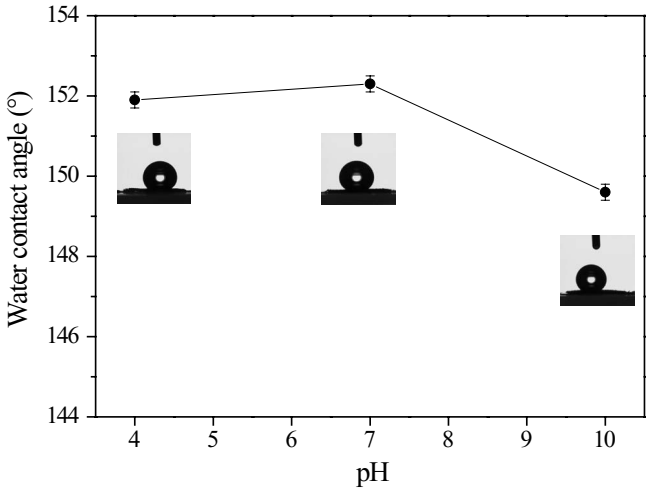

Fig. 13. Static WCAs of the modified nylon mesh in different pH value. The inset images show the shape of the water droplet on each sample.

and the SiO_2 NPs can be coated stably onto the surface of nylon mesh.

3.5. Mechanical property

Generally, the mechanical behavior of oil-water separation membranes is closely related to the intrinsic strength of the materials. Fig. 14 presents the tensile stress-strain curves of the nylon mesh before and after modification. The tensile strength of the original nylon mesh is observed to be 50.6 MPa. Due to the high temperature during the modification process, the tensile strength has been reduced sharply to 13.7 MPa. However, it should be pointed out that this mechanical strength value is still adequate for filtration application.

The robust flexibility of both pristine and modified nylon mesh is proved by a facile bending examination, showing no crack during the operation in Fig. 15.

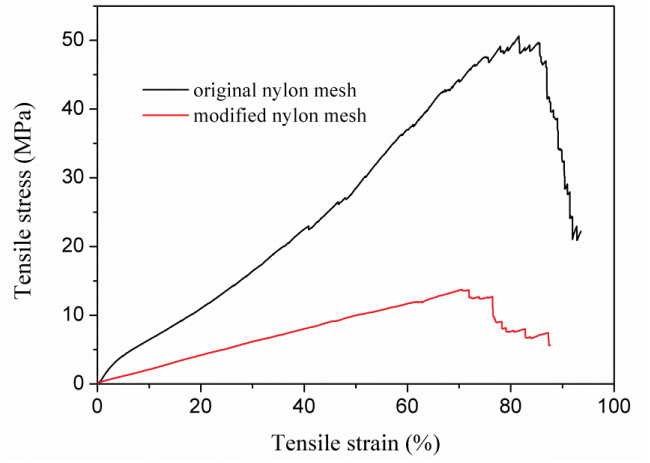

Fig. 14. Stress-strain curves of nylon mesh before and after modification.

Fig. 15. Optical photographs show the robust flexibility of pristine and modified nylon mesh.

4. Conclusions

A facile and cost-effective generalized strategy using environmentally friendly polybenzoxazine and silica nanoparticles has been employed for the engineering of nylon mesh for oil-water separation. The modified nylon mesh exhibited a high water contact angle of 154.3° and a low oil contact angle of 0°. The superhydrophobic-superoleophilic nylon mesh decorated via this strategy can effectively separate the oil-water mixture by gravity with ultrahigh flux ($1.77 \times 10^4 \pm 100$ L/(m^2 h)) and high separation efficiency (99.5% ± 0.1%) in 30-cycle tests. Consequently, it is believed that this strategy can be utilized as a convenient and powerful tool to engineer superhydrophobic-superoleophilic materials for practical applications.

Acknowledgment

The authors would like to acknowledge the financial support from the Senior talents fund of Jiangsu University (12JDG088) and Jiangsu Planned Projects for Postdoctoral Research Funds (1301059B).

Symbols

A	—	Effective area, m^2
g	—	Acceleration of gravity, m/s^2
h_{max}	—	Height, m^2
J	—	Flux, L/(m^2 h)
P_{max}	—	Pressure, Pa
t	—	Time, h
V	—	Volume, L
V_a	—	Volume of collected oil, L
V_0	—	Volume of original oil, L

Greek

ρ	—	Density, kg/m^3
η	—	Separation efficiency, %

Subscripts

a	—	Collected
max	—	Maximum
o	—	Original

References

[1] S. Jamaly, A. Giwa, S.W. Hasan, Recent improvements in oily wastewater treatment: progress, challenges, and future opportunities, J. Environ. Sci., 37 (2015) 15–30.

[2] V. da N. Medeiros, T.C. de Carvalho, E.M. Araújo, H.L. Lira, A.M.D. Leite, E.A.S. dos Santos Filho, Polyethersulfone nanocomposite membranes with different montmorillonite clays for oil/water separation, Desal. Water Treat., 154 (2019) 63–71.

[3] Z.X. Xue, X.W. Xing, S.X. Zhu, W. Zhang, L.Y. Luan, Y.Z. Niu, L.J. Bai, H. Chen, Q. Tao, Underwater superoleophobic porous hydrogel film prepared by soluble salt-template method for oil/water separation in complex environments, Desal. Water Treat., 164 (2019) 151–161.

[4] M.P. Wolf, G.B. Salieb-Beugelaar, P. Hunziker, PDMS with designer functionalities—properties, modifications strategies, and applications, Prog. Polym. Sci., 83 (2018) 97–134.

[5] D.S. Yuan, T. Zhang, Q. Guo, F.X. Qiu, D.Y. Yang, Z.P. Ou, A novel hierarchical hollow SiO_2@MnO_2 cubes reinforced elastic polyurethane foam for the highly efficient removal of oil from water, Chem. Eng. J., 327 (2017) 539–547.

[6] J.Y. Wu, C.W. Huang, P.S. Tsai, Preparation of poly [3-(methacryloylamino) propyl] trimethylammonium chloride coated mesh for oil-water separation, Desal. Water Treat., 158 (2019) 301–308.

[7] X.Y. Yue, J.X. Li, T. Zhang, F.X. Qiu, D.Y. Yang, M.W. Xue, In situ one-step fabrication of durable superhydrophobic-superoleophilic cellulose/LDH membrane with hierarchical structure for efficiency oil/water separation, Chem. Eng. J., 328 (2017) 117–123.

[8] T. Yan, H.W. Meng, W.J.H. Hu, F.P. Jia, Superhydrophilicity and underwater superoleophobicity graphene oxide-micro crystalline cellulose complex-based mesh applied for efficient oil/water separation, Desal. Water Treat., 111 (2018) 155–164.

[9] J. Rong, T. Zhang, F.X. Qiu, J.C. Xu, Y. Zhu, D.Y. Yang, Y.T. Dai, Design and preparation of efficient, stable and superhydrophobic copper foam membrane for selective oil absorption and consecutive oil–water separation, Mater. Des., 142 (2018) 83–92.

[10] J.H. Zhang, Y.W. Shao, C.-T. Hsieh, Y.-F. Chen, T.-C. Su, J.-P. Hsu, R.-S. Juang, Synthesis of magnetic iron oxide nanoparticles onto fluorinated carbon fabrics for contaminant removal and oil-water separation, Sep. Purif. Technol., 174 (2017) 312–319.

[11] E. Karimi, S.S. Barekati, A. Raisi, A. Aroujalian, High-flux electrospun polyvinyl alcohol microfiltration nanofiber membranes for treatment of oil water emulsion, Desal. Water Treat., 147 (2019) 20–30.

[12] J. Bhadra, N.J. Al-Thani, A. Abdulkareem, The effect of electro spinning parameters on polystyrene nanofiber morphology: oil-water separation, Desal. Water Treat., 111 (2018) 146–154.

[13] J. Yang, L.T. Yin, H. Tang, H.J. Song, X.N. Gao, K. Liang, C.S. Li, Polyelectrolyte-fluorosurfactant complex-based meshes with superhydrophilicity and superoleophobicity for oil/water separation, Chem. Eng. J., 268 (2015) 245–250.

[14] X.Y. Zhang, C.Q. Wang, X.Y. Liu, J.H. Wang, C.Y. Zhang, Y.L. Wen, PVA/SiO_2-coated stainless steel mesh with superhydrophilic-underwater superoleophobic for efficient oil-water separation, Desal. Water Treat., 126 (2018) 157–163.

[15] M. Khosravi, S. Azizian, R. Boukherroub, Efficient oil/water separation by superhydrophobic Cu_xS coated on copper mesh, Sep. Purif. Technol., 215 (2019) 573–581.

[16] M. Khosravi, S. Azizian, Synthesis of a novel highly oleophilic and highly hydrophobic sponge for rapid oil spill cleanup, ACS Appl. Mater. Interfaces, 7 (2015) 25326–25333.

[17] L.J. Wang, T.H. Zhang, H.W. Meng, T. Yan, G.Q. Zhao, C.F. Li, F.P. Jiao, J. Huang, Facile fabrication of super-hydrophobic and super-oleophilic Ota-PDA-PU sponge for efficient oil/water separation, Desal. Water Treat., 164 (2019) 144–150.

[18] K.Q. Zhou, G. Tang, R. Gao, S.D. Jiang, In situ growth of 0D silica nanospheres on 2D molybdenum disulfide nanosheets: towards reducing fire hazards of epoxy resin, J. Hazard. Mater., 344 (2018) 1078–1089.

[19] D.S Yuan, T. Zhang, Q. Guo, F.X. Qiu, D.Y. Yang, Z.P. Ou, Recyclable biomass carbon@SiO_2@MnO_2 aerogel with hierarchical structures for fast and selective oil-water separation, Chem. Eng. J., 351 (2018) 622–630.

[20] X.J. Yue, T. Zhang, D.Y. Yang, F.X. Qiu, Z.D. Li, Hybrid aerogels derived from banana peel and waste paper for efficient oil absorption and emulsion separation, J. Cleaner Prod., 199 (2018) 411–419.

[21] J. Rong, F.X. Qiu, T. Zhang, X.Y. Zhang, Y. Zhu, J.C. Xu, D.Y. Yang, Y.T. Dai, A facile strategy toward 3D hydrophobic composite resin network decorated with biological ellipsoidal structure rapeseed flower carbon for enhanced oils and organic solvents selective absorption, Chem. Eng. J., 322 (2017) 397–407.

[22] Y.B. Wei, H. Qi, X. Gong, S.F. Zhao, Specially wettable membranes for oil–water separation, Adv. Mater. Interfaces, 5 (2018) 1800576–1800603.

[23] X.J. Yue, Z.D. Li, T. Zhang, D.Y. Yang, F.X. Qiu, Design and fabrication of superwetting fiber-based membranes for oil/water separation applications, Chem. Eng. J., 364 (2019) 292–309.

[24] W.F. Zhang, N. Liu, Y.Z. Cao, Y.N. Chen, L.X. Xu, X. Lin, L. Feng, A solvothermal route decorated on different substrates: controllable separation of an oil/water mixture to a stabilized nanoscale emulsion, Adv. Mater., 27 (2015) 7349–7355.

[25] F.Z. Chen, J.L. Song, Z.A. Liu, J.Y. Liu, H.X. Zheng, S. Huang, J. Sun, W.J. Xu, X. Liu, Atmospheric pressure plasma functionalized polymer mesh: an environmentally friendly and efficient tool for oil/water separation, ACS Sustainable Chem. Eng., 4 (2016) 6828–6837.

[26] B. Shang, Y.B. Wang, B. Peng, Z.W. Deng, Bioinspired polydopamine particles-assisted construction of superhydrophobic surfaces for oil/water separation, J. Colloid Interface Sci., 482 (2016) 240–251.

[27] B.B. Li, X.Y. Zhang, Superhydrophobic nylon cloth coated with modified silica used for oil-water separation, Environ. Prog. Sustainable Energy, 38 (2019) e13051.

[28] J. Liu, X. Lu, Z. Xin, C.L. Zhou, Synthesis and surface properties of low surface free energy silane-functional polybenzoxazine films, Langmuir, 29 (2013) 411–416.

[29] L. Shen, H.L. Ding, W. Wang, Q.P. Guo, Fabrication of Ketjen black-polybenzoxazine superhydrophobic conductive composite coatings, Appl. Surf. Sci., 268 (2013) 297–301.

[30] Y.-L. Liao, C.-C. Hu, J.-Y. Lai, Y.-L. Liu, Crosslinked polybenzoxazine based membrane exhibiting *in-situ* self-promoted separation performance for pervaporation dehydration on isopropanol aqueous solutions, J. Membr. Sci., 531 (2017) 10–15.

[31] C.-T. Liu, Y.-L. Liu, pH-induced switches of the oil- and water-selectivity of crosslinked polymeric membranes for gravity-driven oil-water separation, J. Mater. Chem. A, 4 (2016) 13543–13548.

[32] H.-Y. Li, G.-A. Li, Y.-Y. Lee, H.-Y. Tuan, Y.-L. Liu, A thermally stable, combustion-resistant, and highly ion-conductive separator for lithium-ion batteries based on electrospun fiber mats of crosslinked polybenzoxazine, Energy Technol., 4 (2016) 551–557.

[33] T. Agag, A. Akelah, A. Rehab, S. Mostafa, Flexible polybenzoxazine thermosets containing pendent aliphatic chains, Polym. Int., 61 (2012) 124–128.

[34] H. Zhang, X. Lu, Z. Xin, W.F. Zhang, C.L. Zhou, Preparation of superhydrophobic polybenzoxazine/SiO_2 films with self-cleaning and ice delay properties, Prog. Org. Coat., 123 (2018) 254–260.
[35] X.J. Yue, T. Zhang, D.Y. Yang, F.X. Qiu, Z.D. Li, Y. Zhu, H.Q. Yu, Oil removal from oily water by a low-cost and durable flexible membrane made of layered double hydroxide nanosheet on cellulose support, J. Cleaner Prod., 180 (2018) 307–315.
[36] C. Zhang, D.Y. Yang, T. Zhang, F.X. Qiu, Y.T. Dai, J.C. Xu, Z.F. Jing, Synthesis of MnO_2/poly(*n*-butylacrylate-*co*-butyl methacrylate-*co*-methyl methacrylate) hybrid resins for efficient oils and organic solvents absorption, J. Cleaner Prod., 148 (2017) 398–406.
[37] X.J. Yue, T. Zhang, D.Y. Yang, F.X. Qiu, J. Rong, J.C. Xu, J.S. Fang, The synthesis of hierarchical porous Al_2O_3/acrylic resin composites as durable, efficient and recyclable absorbents for oil/water separation, Chem. Eng. J., 309 (2017) 522–531.